

***Near-infrared diffuse optical imaging for early prediction of breast cancer response to neoadjuvant chemotherapy: a comparative study using FDG-PET/CT***

**Authors**

Shigeto Ueda<sup>1</sup>, Nobuko Yoshizawa<sup>2</sup>, Takashi Shigekawa<sup>1</sup>, Hideki Takeuchi<sup>1</sup>,  
Hiroyuki Ogura<sup>3</sup>, Akihiko Osaki<sup>1</sup>, Toshiaki Saeki<sup>1</sup>, Yukio Ueda<sup>4</sup>, Tomohiko Yamane<sup>5</sup>,  
Ichiei Kuji<sup>5</sup>, Harumi Sakahara<sup>2</sup>

**Affiliations**

1. Department of Breast Oncology, International Medical Center, Saitama Medical University, 1371-1 Yamane, Hidaka, 350-1298, Japan

2. Department of Diagnostic Radiology and Nuclear Medicine, Hamamatsu University, School of Medicine, 1-20-1 Handayama, Hamamatsu, 431-3192, Japan

3. Department of Breast Surgery, Hamamatsu University, School of Medicine, 1-20-1 Handayama, Hamamatsu, 431-3192, Japan

4. Central Research Laboratory, Hamamatsu Photonics K.K., 5000, Hamakitaku, Hamamatsu, 434-8601, Japan

5. Department of Nuclear Medicine, International Medical Center, Saitama Medical

University, 1371-1 Yamane, Hidaka, 350-1298, Japan

Key words: optical imaging, breast cancer, chemotherapy, FDG-PET

Corresponding author, Shigeto Ueda

E-mail: [syueda@saitama-med.ac.jp](mailto:syueda@saitama-med.ac.jp)

Tel: +81-42-984-4670 (Ext. 8758); Fax: +81-42-984-4672

Disclaimer: The authors indicated no potential conflicts of interest.

Financial support: JSPS KAKEN grants (25830105 and 26282144) and 2016

Hidaka research grant.

Word count: 4636

Running Title: Optical imaging of cancer chemotherapy

Key words: optical imaging, hemoglobin, neoadjuvant chemotherapy, breast cancer, FDG-PET

## ABSTRACT

Purpose: Diffuse optical spectroscopic imaging (DOSI) is used as an indicator of tumor blood volume quantified by tissue hemoglobin concentrations. We aimed to determine whether early changes in tumor total hemoglobin (tHb) concentration can predict a pathological complete response (pCR) to neoadjuvant chemotherapy (NAC) in patients with operable breast cancer, and we compared the predictive value of pCR between DOSI and 2-deoxy-2-<sup>18</sup>F-fluoro-D-glucose (FDG) positron emission tomography (PET) combined with computed tomography (CT).

Methods: Of the 100 patients enrolled, 84 patients were prospectively evaluated for primary objective analysis. Sixty four of the patients underwent both sequential DOSI scans at baseline after their first and second chemotherapy courses and FDG-PET/CT at baseline and after their second chemotherapy course. The mean tHb (tHb<sub>mean</sub>) concentration and maximum standardized uptake values (SUV<sub>max</sub>) of the lesion were measured using DOSI and FDG-PET/CT, respectively, and the percentage change in tHb<sub>mean</sub> ( $\Delta$ tHb<sub>mean</sub>) and change in SUV<sub>max</sub> ( $\Delta$ SUV<sub>max</sub>) were calculated. We compared the diagnostic performances of DOSI and FDG-PET/CT for predicting pCR via the analysis of the receiver operating characteristic curves.

Results: pCR was achieved in 16 patients, and NAC caused a significant reduction of  $\Delta\text{tHb}_{\text{mean}}$  in pCR compared with non-pCR after the two chemotherapy courses.

Using the tentative  $\Delta\text{tHb}_{\text{mean}}$  cutoff values after the first and second courses, the ability to predict pCR was as follows: sensitivity 81.2%, specificity 47.0% and sensitivity 93.7%, specificity 47.7%, respectively. Comparison of the diagnostic performances of DOSI and FDG-PET/CT revealed areas under the curve (AUCs) of 0.69 and 0.75 of  $\Delta\text{tHb}_{\text{mean}}$  after the first and second courses, respectively, which were lower than those of  $\Delta\text{SUV}_{\text{max}}$  (0.90).

Conclusion: DOSI predicted pCR in patients with breast cancer with moderate accuracy. The diagnostic performance of DOSI was inferior to that of the early metabolic response as monitored by FDG-PET/CT.

## INTRODUCTION

NAC has been established as the standard of care for patients with locally advanced breast cancer (1). Although it is increasingly used in early breast cancer depending on the histological subtype, further predictive tools are required as companion diagnostics to identify and treat patients with responsive disease.

Biofunctional imaging techniques for early response assessment may soon change the process of cancer management. Presently, 2-deoxy-2-<sup>18</sup>F-fluoro-D-glucose (FDG) positron emission tomography (PET) combined with computed tomography (CT) is accepted as a noninvasive method for the early evaluation of the response to therapy because decreased glucose metabolism precedes tumor shrinkage (2). However, the expensive technology using FDG-PET/CT during NAC has precluded its integration into clinical practice (3). Near-infrared optical imaging based on the visualization of the hemodynamic status of the tissue [such as oxyhemoglobin (O<sub>2</sub>Hb) and deoxyhemoglobin (HHb) concentrations] is reportedly promising for determining the physiological status of tumor-bearing breast tissue and for monitoring early responses (4).

We recently established a time-resolved (TR)-diffuse optical spectroscopic

imaging (DOSI) system (TRS20; Hamamatsu Inc., Hamamatsu, Japan) for breast measurement and reported that elevation of the total hemoglobin (tHb) concentration in lesions compared with that of the background normal tissue reflects hypervascularity of the lesion (5). We hypothesized that changes in lesional tHb concentrations would indicate the degree of tumor angiogenesis during treatment, thereby predicting the therapeutic response.

Several recent studies have revealed that decreased lesional tHb concentrations observed on longitudinal DOSI scans can accurately distinguish pathological responders to cytotoxic chemotherapy from others (6,7).

Therefore, we aimed to prospectively evaluate the diagnostic performance of sequential TR-DOSI scans for monitoring early chemotherapy response and primarily to determine whether changes in lesional tHb concentration measured after the first and second courses of cytotoxic drug administration can predict pCR in patients with primary breast cancer. Secondly, we compared the diagnostic performances of TR-DOSI and FDG-PET/CT for predicting pCR.

## **MATERIALS AND METHODS**

## Patient eligibility

Patients aged >18 years who had newly diagnosed, biopsy-proven breast cancer, clinical stage T1c-4, N0-2 primary breast cancer according to the TNM classification (6<sup>th</sup> edition), and planned to undergo at least four chemotherapy cycles were eligible for this prospective TR-DOSI chemotherapy monitoring study.

The exclusion criteria included pregnancy, previous breast cancer treatment, bilateral breast cancer, or ineligibility for surgery. Patients enrolled at Saitama Medical University and Hamamatsu University, School of Medicine, participated in our TR-DOSI study. The institutional review board at each of these centers approved this study, and written informed consent was obtained from each patient.

The study was conducted in accordance with the Declaration of Helsinki and was registered at the UMIN Clinical Trials Registry (no. 000011888). The physicians determined a standard-of-care chemotherapy regimen for each patient according to the patient's age, cancer stage, and tumor subtype. All patients underwent breast-conserving surgery or a mastectomy with sentinel node biopsy and/or axillary dissection after completing their courses of chemotherapy.

## Study design

All patients in this study had previously undergone a mammogram, ultrasound (US) and/or contrast-enhanced magnetic resonance imaging (MRI).

TR-DOSI was performed prior to treatment and after the first and second infusions of the anticancer drug (Fig. 1). Only patients with clearly visible lesions on US were considered evaluable and underwent sequential TR-DOSI scans. In our study, measurements were obtained an average of 18 days (range, 14–30 days) after the core biopsy and at day –2 to day 1 before the initial infusion of the anticancer drug. The subsequent assessments were taken at day –2 to day 1 before the second or third drug infusions. The patients also underwent FDG-PET/CT scans (Biograph 6/16; Siemens, Berlin, Germany) at baseline and 2–3 weeks after the second course of NAC.

## TR-DOSI scan protocol

The system has been described previously in detail (8). In brief, after locating the tumor by US, a grid was manually drawn using a marker pen, mapping 7 × 7 points with 10-mm intervals between the points in the x–y dimension, with the tumor



located at the center of the grid. A handheld probe with a 2.8-cm source-detector distance was brought into contact with each point on the breast, thus measuring the optical properties of the tissue at each point. The contralateral normal breast was also measured as a reference.

The imaging systems at the two institutions were confirmed to have comparable imaging quality and data acquisition capability before the start of the study. After subtracting water and lipid absorption (using the estimate that normal breast tissue comprises 18.7% water and 66.1% lipid) (9), tissue concentrations ( $\mu\text{M}$ ) of  $\text{O}_2\text{Hb}$  and HHb were calculated from the absorption coefficient at wavelengths of 760, 800, and 830 nm. The tHb concentration was recorded as the sum of  $\text{O}_2\text{Hb}$  and HHb. The percentage of tissue oxygen saturation was defined as the ratio between the concentrations of  $\text{O}_2\text{Hb}$  and tHb ( $\text{O}_2\text{Hb}/\text{tHb} \times 100$ ). The region of interest (ROI; a circle measuring 2 cm in radius) was assigned to the skin, including the area of the target lesion and the adjacent normal tissue. In total, 10–14 points were included for each ROI. We set the ROI showing the highest concentration of tHb above the lesion as identified by US. After completing all imaging studies, the optical images acquired at baseline and after the first and second courses of

chemotherapy were analyzed by two investigators (SU and NY) blinded to all medical and pathological reports. The percent change in the mean tHb ( $\Delta tHb_{\text{mean}}$ ) between the baseline and after chemotherapy was calculated as follows:  $(\text{post-therapeutic } tHb_{\text{mean}} - \text{baseline } tHb_{\text{mean}}) / \text{baseline } tHb_{\text{mean}} \times 100 (\%)$ .

#### FDG-PET/CT scan procedure

Patients with a clearly visible lesion at the baseline assessment underwent serial FDG-PET/CT scans. The imaging protocol was designed to ensure standardized uptake value (SUV) measurements across all time points. Blood glucose levels were measured in all patients before FDG administration; none had blood glucose levels exceeding 200 mg/dl. After fasting for at least 6 h, the patients received an intravenous injection of FDG (3.7–4.0 MBq/kg). After a 60-min uptake period, all image acquisitions were performed from the thigh level to the skull base with the arms raised using a PET/CT system combined with a 6- or 16-slice CT scanner. PET emission data were acquired in the three-dimensional mode (2 min per bed position) and reconstructed using ordered subsets expectation maximization. Tumor FDG uptake was quantified by SUV, which normalizes the measured tissue

activity in an ROI by the injected dose and body weight, calculated by the tracer concentration per the following equation: (Bq/ml)/(injected activity (Bq)/patient body weight (g)).

All the PET/CT images were interpreted by experienced nuclear medicine physicians (HS, TY, and IK) who were blinded to all medical and pathological information. When a hypermetabolic lesion was detected on PET/CT, the maximum SUV ( $SUV_{max}$ ) was prospectively calculated, and the percent change in  $\Delta SUV_{max}$  was calculated as follows:  $(\text{post-therapeutic } SUV_{max} - \text{baseline } SUV_{max}) / \text{baseline } SUV_{max} \times 100 (\%)$ .

#### Histopathological response

Resected surgical specimens were used as the reference standard for determining the residual disease status. The surgical specimens were cut into 0.5-cm-thick slices, fixed in 10% neutral-buffered formalin, and processed for histological examination. For routine clinical practice, all slides sectioned from the paraffin-embedded blocks were reviewed and reported on with respect to residual cancer cellularity, *in situ* disease, and the number of lymph nodes involved.

At least two experienced pathologists meticulously reviewed all surgical specimens and reached a consensus. A histopathological response was assessed by applying the grading criteria to definitive surgery specimens in comparison with the initial core biopsy samples. The meta-analysis from Cortazar *et al.* showed that only pCR, defined as the absence of invasive cancer cells in the primary tumor and in lymph nodes, is associated with improved patient survival (10). In this study, however, we defined the primary endpoint of pCR as the absence of invasive cancer cells in the breast irrespective of the presence of lymph node infiltration by malignant cells (ypT0/is) (11). All other cases were classified as non-pCR.

#### Statistical analysis

Student's *t*-test was used when the data followed a normal distribution.

Otherwise, the nonparametric Mann–Whitney *U*-test was used. The chi-square test was performed to analyze the associations between two categorical variables. To identify an optimal threshold for pCR prediction, receiver operating characteristic (ROC) curve analysis was performed by incrementally increasing the cutoff values. The area under the curve (AUC), sensitivity, specificity, positive predictive value

(PPV), negative predictive value (NPV), and accuracy were obtained from the ROC curve analysis. A  $P \leq 0.05$  was considered statistically significant. Data were analyzed using statistics software (Version 15.2.2; MedCalc, Ostend, Belgium).

## RESULTS

### Patients

Of the 100 patients who were enrolled between September 2013 and February 2015 from the two institutes, a total of 84 patients (84%) were included in TR-DOSI study and a total of 64 patients (64%) were included in a comparison study of TR-DOSI and FDG-PET, and the patient characteristics are shown in Table 1. The number of patients included in each analysis was summarized in Supplemental figure. After completing chemotherapy, 39 patients (46.4%) underwent breast-conserving surgery. Histopathology revealed pCR in 16 (19%) and non-pCR in 68 (81%) of the 84 patients. pCR tumors had significantly higher frequency of hormone-receptor negativity or HER2 positivity than non-pCR tumors ( $p = 0.003$ ). No difference was observed between pCR and non-pCR tumors with respect to patient age, tumor size, histology, or axillary involvement. The mean tumor depth

from the skin as seen by US was 6.8 mm (range 0–17.3 mm). The chemotherapy regimens administered in this study, including the doses and schedules, are summarized in Table 2.

#### Hemodynamic response with TR-DOSI

The first TR-DOSI scan was performed at a median of –1 days (range, –2 to 1 days) before the first infusion. No significant differences were found in the baseline hemoglobin parameters between pCR and non-pCR irrespective of the intrinsic subtypes (Supplemental Table). The second and third scans were performed at a mean of 25.1 days  $\pm$  7.2 (SD) and at a mean of 48.8 days  $\pm$  11.7 (SD) after the first infusion, respectively. Representative optical images of lesional tHb from three different subjects at baseline and after the first and second chemotherapy courses are shown in Figure 2. Figure 3A shows  $\Delta tHb_{mean}$  during chemotherapy in pCR and non-pCR lesions. pCR tumors showed a significantly larger decrease in  $\Delta tHb_{mean}$  after the first chemotherapy course (first-course  $\Delta tHb_{mean}$ ) than did non-pCR tumors (mean, –23.4%  $\pm$  4.3 SE vs. mean, –14.1%  $\pm$  1.7 SE;  $p = 0.02$ ) and after the second chemotherapy course (second-course  $\Delta tHb_{mean}$ ) (mean, –33.9%  $\pm$  3.8

SE vs. mean,  $-20.2\% \pm 1.7$  SE;  $p = 0.001$ ). Figure 3B compares the absolute value  $tHb_{\text{mean}}$  between pCR and non-pCR lesions. The  $tHb_{\text{mean}}$  at baseline and after the first course did not differ between pCR and non-pCR tumors (baseline: median 31.1, 95% CI 25.7–49.8 vs. median 33.5, 95% CI 31.2–38.3;  $p = 0.4$  and first course: median 23.8, 95% CI 20.8–31.5 vs. median 29.8, 95% CI 27.8–31.9;  $p = 0.06$ ). The second-course  $tHb_{\text{mean}}$  differed significantly between pCR and non-pCR tumors (median 19.9, 95% CI 16.8–27.3 vs. median 28.0, 95% CI 24.4–31.2;  $p = 0.02$ ). The ability to predict pCR was as follows: sensitivity 81.2%, specificity 47.0%, PPV 26.5%, NPV 91.4%, and accuracy 53.5%, with an optimal cutoff value of  $-12.4\%$  for the first-course  $\Delta tHb_{\text{mean}}$  and sensitivity 93.7%, specificity 47.7%, PPV 30.0%, NPV 96.9%, and accuracy 56.6%, with an optimal cutoff value of  $-20.5\%$  for the second-course  $\Delta tHb_{\text{mean}}$ .

#### Metabolic response with FDG-PET/CT

Of the 69 patients who agreed to participate in the PET study and underwent sequential FDG-PET/CT scans, 64 (92.7%) patients who had tumor  $SUV_{\text{max}} > 3.0$  at baseline were evaluated for PET-guided monitoring of their response to treatment

(3). The patients' distribution between the two studies were similar (Table 1). A significant decrease in  $\Delta\text{SUV}_{\text{max}}$  was observed in pCR tumors compared with that of non-pCR tumors (mean,  $-72.5\% \pm 3.5 \text{ SE}$  vs.  $-35.6\% \pm 3.4 \text{ SE}$ ;  $p < 0.0001$ ). For an optimal threshold of  $\Delta\text{SUV}_{\text{max}}$  set at  $-53.3\%$ , the diagnostic performance for predicting pCR was as follows: sensitivity 100%, specificity 77.7%, PPV 55.5%, and NPV 100%. The diagnostic accuracy was 82.6%.

#### Comparison of TR-DOSI with FDG-PET/CT

Comparison of the diagnostic performance for predicting pCR between TR-DOSI  $\Delta\text{tHb}_{\text{mean}}$  and FDG-PET/CT  $\Delta\text{SUV}_{\text{max}}$  using ROC curve analysis indicated that the AUCs of both first- and second-course  $\Delta\text{tHb}_{\text{mean}}$  were inferior to that with  $\Delta\text{SUV}_{\text{max}}$  (Fig. 4). There was no significant difference between those of the first- and second-course  $\Delta\text{tHb}_{\text{mean}}$ . Scatter plots showed no significant linear correlation between second-course  $\Delta\text{tHb}_{\text{mean}}$  and  $\Delta\text{SUV}_{\text{max}}$  ( $r = 0.23$ ,  $p = 0.06$ ; Fig. 5). When combined with second-course  $\Delta\text{tHb}_{\text{mean}}$  and  $\Delta\text{SUV}_{\text{max}}$  using an optimal cutoff, the results were as follows: diagnostic accuracy 93.7%, sensitivity 100%, specificity 92.0%, PPV 77.7%, and NPV 100%.



## DISCUSSION

### Early response of optical hemodynamic biomarker

Both the first- and second-course  $\Delta tHb_{mean}$  for the pCR tumors decreased significantly more than that for the non-pCR tumors. In the majority of the pCR tumors, the lesional tHb decreased sharply after beginning chemotherapy and remained at a low level equivalent to that of the background tissue. In contrast,  $\Delta tHb_{mean}$  of non-pCR tumors varied greatly in response to chemotherapy. In half of the non-pCR patients, the tumor tHb concentration decreased by  $-20\%$  or less. Consequently, although the specificity and PPV were low, the high sensitivity and high NPV of this method could help physicians exclude nonresponding patients early on in the course of NAC.

In contrast, baseline hemoglobin parameters, including tHb and oxygen saturation, did not differ between pCR and non-pCR (Supplemental figure). Optical researchers showed that tHb or oxygen saturation of pCR-achieving tumors is significantly higher than that of non-pCR tumors (12,13). This discrepancy may be explained by differences of technology and measurement procedures or physiological variations of the baseline hemoglobin concentration.

## Comparison between TR-DOSI and FDG-PET/CT

Comparison of TR-DOSI and FDG-PET/CT for predicting pCR revealed that the AUC (0.75) after the second-course  $\Delta\text{tHb}_{\text{mean}}$  was inferior to the AUC (0.90) after the second-course  $\Delta\text{SUV}_{\text{max}}$ . This finding indicates that FDG-PET technology is more useful than tHb optical imaging with regard to the early prediction of tumor response. PET Response Criteria in Solid Tumors is still well suited to early prediction of the tumor response to chemotherapy (14). Coudert *et al.* conducted a successful FDG-PET-guided response-adopted randomized trial and revealed that the combination chemotherapy of bevacizumab and trastuzumab plus docetaxel had a higher pCR rate (43.8%) than that (24.0%) of trastuzumab plus docetaxel in HER2-positive breast cancer that was less responsive to trastuzumab based on FDG-PET/CT (15). In metabolic responders treated with trastuzumab plus docetaxel, the pCR rate was close to 54%.

Although optical imaging could be a low-cost alternative to FDG-PET/CT, tHb measurements alone may not be enough to replace tumor glycolysis measurements for predicting histological outcomes. The weak linear correlation ( $r$

= 0.23,  $p = 0.06$ ) we observed between  $\Delta tHb_{\text{mean}}$  and  $\Delta SUV_{\text{max}}$  demonstrates the significance of using multiple parameters to assess the response to chemotherapy (Fig. 5). The combined results from TR-DOSI and FDG-PET/CT distinguished pCR from non-pCR with an accuracy of 93.7%, which was higher than that of either modality alone (FDG-PET/CT accuracy 82.6% and DOSI accuracy 56.6%). This result suggests that the response of breast cancer to chemotherapy is complex and multifactorial; that is, the use of multiparametric and multimodal imaging biomarkers may more precisely stratify the tumor response (16). The present criteria used for histological assessment depends on the degree of cancer cell eradication and tumor shrinkage; however, tumor stromal changes, such as remodeling of the vasculature, are not taken into account. Therefore, a subgroup of patients classified as non-pCR might have responded but simply were not recognized as having responded under the current classification system. Further study is required to clarify whether assessment of early tHb response using TR-DOSI will translate into survival benefits.

#### Study limitations

Further work is required to overcome the limitations of the present study. First, systemic stratification of intrinsic subtypes is recommended when conducting a clinical study because different biological characteristics and administration of targeted drugs may influence tumor vascularity. Previous FDG-PET studies demonstrated that triple-negative breast cancer are more intensely FDG avid than others (17,18). A prospective comparison study stratified by intrinsic subtype with identical regimes for all patients is required. Second, although pCR is a suitable surrogate prognostic marker in patients with breast cancer, a recent meta-analysis of neoadjuvant trials has understated the importance of pCR in patients with luminal tumors (10).

We had three reasons why we defined the primary endpoint as pCR with ypT0/is irrespective of lymph node involvement. First, unlike FDG-PET/CT, TR-DOSI can only measure primary tumors, including the surrounding normal tissue, but cannot detect axillary metastatic lymph nodes. Second, our aim was to evaluate the correlation between early tHb changes of the primary tumor and the histological response of the primary tumor after completion of neoadjuvant chemotherapy. Third, we consider the knowledge of the primary tumor achieving a pCR as still

being informative because the surgeon may decide to perform minimal breast-conserving surgery on the patient.

TR-DOSI and PET comparison study included only 64 patients because some patients refused further exposure to radiation or for financial reasons.

There are several limitations of DOSI technology. First, the measurement of optical absorption is limited to the reach of photons and up to only a few centimeters depth from the skin. The entire tumor blood volume cannot be observed using this approach, which may result in partial volume effects. In addition, the chest wall thickness can be tilted at different angles, thereby compromising the measurement (19). Second, the low sensitivity and poor spatial resolution of this technique may decrease the reproducibility of the results. Some investigators have argued that the use of US- or MRI-guided diffuse optical tomography may provide better results than DOSI alone, which could improve the quality of the study (20,21). Third, no consensus has been reached for determining the ROI of the lesional tHb regarding user and device independence. Fourth, our TR-DOSI cannot assess the tissue content of water and lipid. To improve the

diagnostic accuracy, more data should be acquired at the longer wavelengths that are absorbed by water and lipids.

## **CONCLUSION**

To the best of our knowledge, the present prospective study is the first to demonstrate that the early tHb response of a tumor to chemotherapy can be used to identify pCR with moderate accuracy and with a lower diagnostic performance than the FDG-PET/CT response classification in numerous patients with breast cancer. However, the combination of DOSI and FDG-PET/CT improved the diagnostic performance over that of each modality alone. This noninvasive DOSI technology has the potential to provide complementary information for directing individualized therapy.

## **ACKNOWLEDGMENTS**

We would like to thank Yutaka Yamashita, Motoki Oda, Etsuko Omae, Hiroyuki Suzuki, and Kenji Yoshimoto for technical support; Noriko Wakui for her help with patient measurements; Hiroko Shimada, Ikuko Sugitani, Michiko Sugiyama, and

Eiko Hirokawa for their contribution to patient enrollment; Enago ([www.enago.jp](http://www.enago.jp))  
for the English language review.

## REFERENCES

1. Kaufmann M, von Minckwitz G, Bear HD, et al, Recommendations from an international expert panel on the use of neoadjuvant (primary) systemic treatment of operable breast cancer: new perspectives 2006. *Ann Oncol.* 2007;18:1927-1934.
2. Mghanga FP, Lan X, Bakari KH, et al, Fluorine-18 fluorodeoxyglucose positron emission tomography-computed tomography in monitoring the response of breast cancer to neoadjuvant chemotherapy: a meta-analysis. *Clin Breast Cancer.* 2013;13:271-279.
3. Kurland BF, Doot RK, Linden HM, et al, Multicenter trials using (1)(8)F-fluorodeoxyglucose (FDG) PET to predict chemotherapy response: effects of differential measurement error and bias on power calculations for unselected and enrichment designs. *Clin Trials.* 2013;10:886-895.
4. Tromberg BJ, Cerussi A, Shah N, et al, Imaging in breast cancer: diffuse optics in breast cancer: detecting tumors in pre-menopausal women and monitoring neoadjuvant chemotherapy. *Breast Cancer Res.* 2005;7:279-285.
5. Ueda S, Nakamiya N, Matsuura K, et al, Optical imaging of tumor vascularity associated with proliferation and glucose metabolism in early breast cancer: clinical application of total hemoglobin measurements in the breast. *BMC Cancer.* 2013;13:514-523.
6. Cerussi A, Hsiang D, Shah N, et al, Predicting response to breast cancer neoadjuvant chemotherapy using diffuse optical spectroscopy. *Proc Natl*



*Acad Sci U S A.* 2007;104:4014-4019.

7. Jiang S, Pogue BW, Kaufman PA, et al, Predicting breast tumor response to neoadjuvant chemotherapy with diffuse optical spectroscopic tomography prior to treatment. *Clin Cancer Res.* 2014;20:6006-6015.
8. Oda M, Yamashita Y, Nishimura G, et al, A simple and novel algorithm for time-resolved multiwavelength oximetry. *Phys Med Biol.* 1996;41:551-562.
9. Cerussi A, Shah N, Hsiang D, et al, In vivo absorption, scattering, and physiologic properties of 58 malignant breast tumors determined by broadband diffuse optical spectroscopy. *J Biomed Opt.* 2006;11:044005-0440014.
10. Cortazar P, Zhang L, Untch M, et al, Pathological complete response and long-term clinical benefit in breast cancer: the CTNeoBC pooled analysis. *Lancet.* 2014;384:164-172.
11. Bear HD, Anderson S, Smith RE, et al, Sequential preoperative or postoperative docetaxel added to preoperative doxorubicin plus cyclophosphamide for operable breast cancer:national surgical adjuvant breast and bowel project protocol B-27. *J Clin Oncol.* 2006;24:2019-2027.
12. Ueda S, Roblyer D, Cerussi A, et al, Baseline tumor oxygen saturation correlates with a pathologic complete response in breast cancer patients undergoing neoadjuvant chemotherapy. *Cancer Res.* 2012;72:4318-4328.
13. Zhu Q, DeFusco PA, Ricci A, Jr., et al, Breast cancer: assessing response to neoadjuvant chemotherapy by using US-guided near-infrared

tomography. *Radiology*. 2013;266:433-442.

14. Wahl RL, Jacene H, Kasamon Y, et al, From RECIST to PERCIST: Evolving Considerations for PET response criteria in solid tumors. *J Nucl Med*. 2009;50 Suppl 1:122S-150S,

15. Coudert B, Pierga JY, Mouret-Reynier MA, et al, Use of [(18)F]-FDG PET to predict response to neoadjuvant trastuzumab and docetaxel in patients with HER2-positive breast cancer, and addition of bevacizumab to neoadjuvant trastuzumab and docetaxel in [(18)F]-FDG PET-predicted non-responders (AVATAXHER): an open-label, randomised phase 2 trial. *Lancet Oncol*. 2014;15:1493-1502.

16. Specht JM, Kurland BF, Montgomery SK, et al, Tumor metabolism and blood flow as assessed by positron emission tomography varies by tumor subtype in locally advanced breast cancer. *Clin Cancer Res*. 2010;16:2803-2810.

17. Koolen BB, Pengel KE, Vogel WV, et al, FDG PET/CT during neoadjuvant chemotherapy may predict response in ER-positive/HER2-negative and triple negative, but not in HER2-positive breast cancer. *Breast*. 2013 ;22:691-697.

18. Groheux D, Majdoub M, Sanna A, et al, Early Metabolic Response to Neoadjuvant Treatment: FDG PET/CT Criteria according to Breast Cancer Subtype. *Radiology*. 2015;277:358-371.

19. Ardeshirpour Y, Zhu Q, Optical tomography method that accounts for tilted chest wall in breast imaging. *J Biomed Opt*. 2010;15:041515-041523.

20. Carpenter CM, Srinivasan S, Pogue BW, et al, Methodology development for three-dimensional MR-guided near infrared spectroscopy of breast tumors. *Opt Express*. 2008;16:17903-17914.

21. Zhu Q, Hegde PU, Ricci A, Jr., et al, Early-stage invasive breast cancers: potential role of optical tomography with US localization in assisting diagnosis. *Radiology*. 2010;256:367-378.

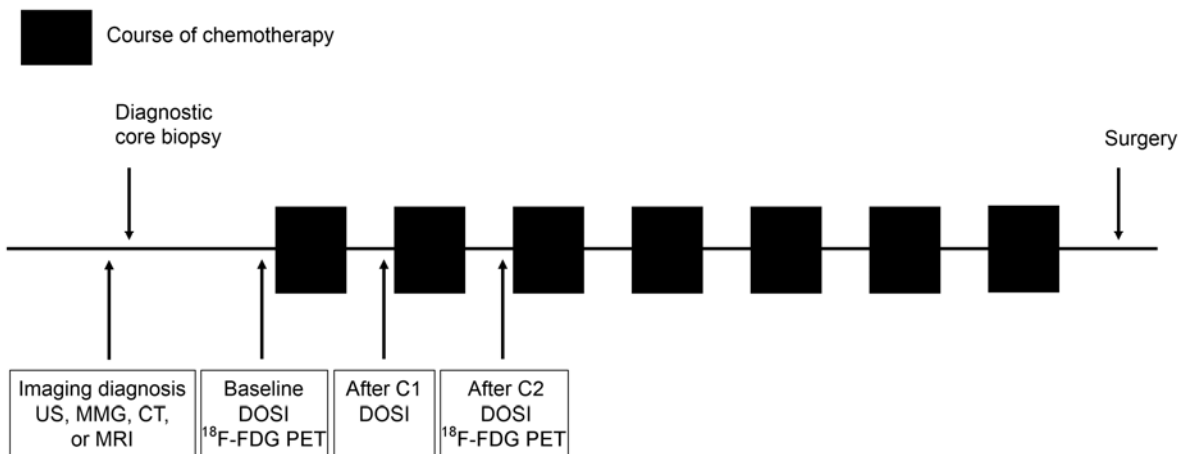


**Figure 1.** Longitudinal imaging study with FDG-PET and DOSI. C1, the first chemotherapy course; C2, the second chemotherapy course; US, ultrasound; MMG, mammography; CT, computed tomography; MRI, magnetic resonance imaging; DOSI, diffuse optical spectroscopic imaging; FDG, 2-deoxy-2-<sup>18</sup>F-fluoro-D-glucose; PET, positron emission tomography.

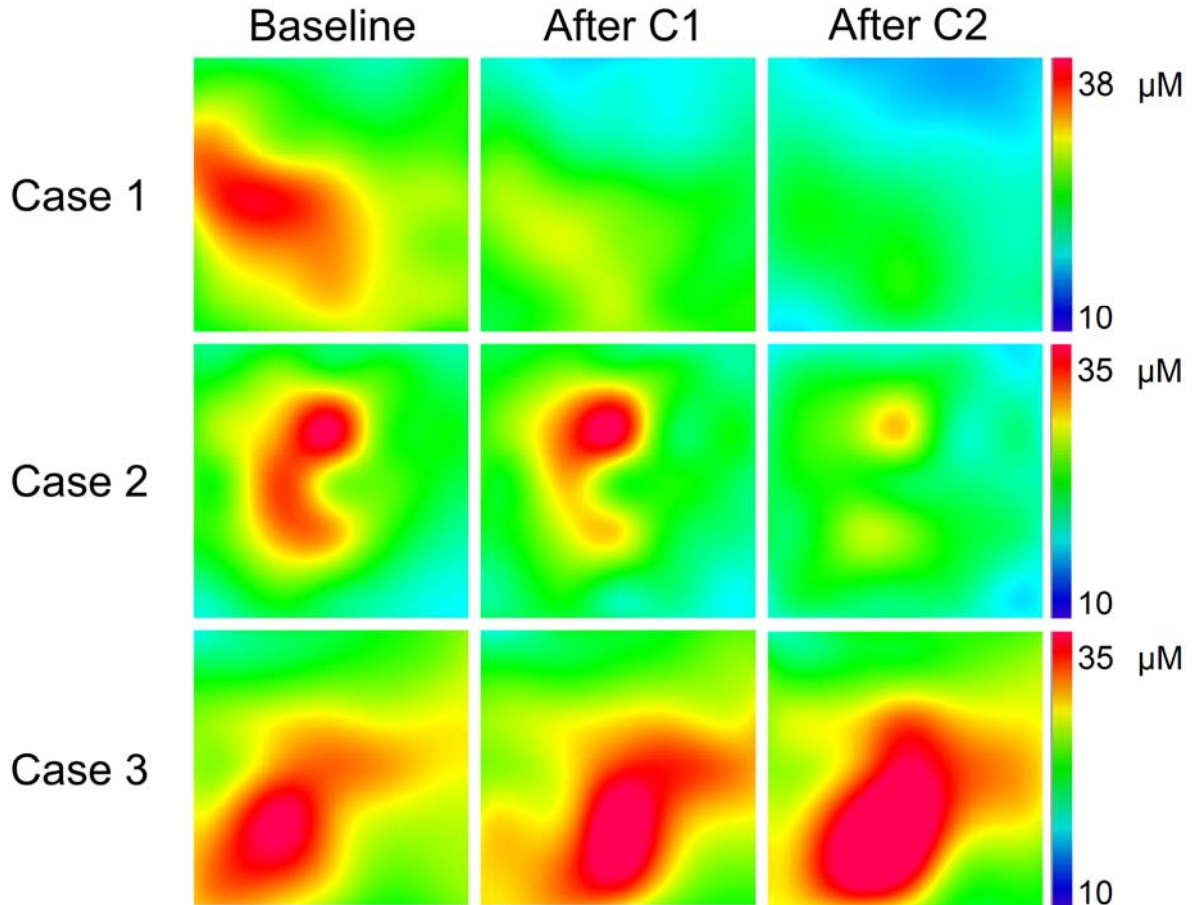


**Figure 2.** Lesional total hemoglobin maps from three different subjects at baseline, after C1, and after C2. Each map shows a 60 mm × 60 mm measurement area that includes the tumor and the surrounding normal margin. Top: an example of pCR. The tumor size was 22.0 mm before chemotherapy. Middle: an example of a 47.0-mm tumor that partially responded to chemotherapy. Bottom: an example of a 24.2-mm tumor that did not respond to chemotherapy. C1, the first chemotherapy course; C2, the second chemotherapy course.

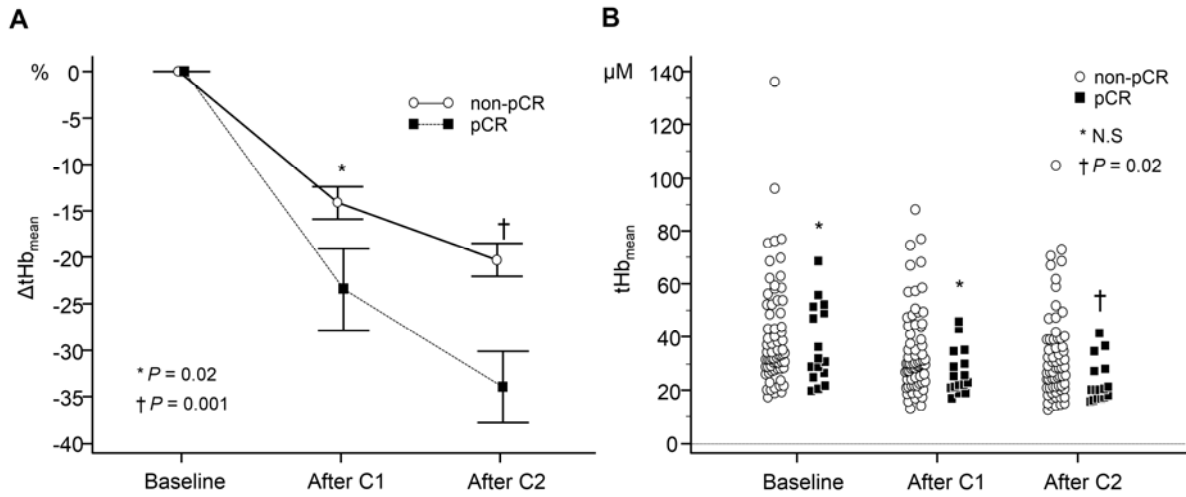


**Figure 3.** Change in  $tHb_{mean}$  ( $\Delta tHb_{mean}$ ) during neoadjuvant chemotherapy in pCR and non-pCR (**A**). Absolute value of  $tHb_{mean}$  concentration at baseline, after C1, and after C2 in pCR and non-pCR (**B**). The chi-square test was performed. C1, the first chemotherapy course; C2, the second chemotherapy course;  $tHb_{mean}$ , mean value of the total hemoglobin concentration.

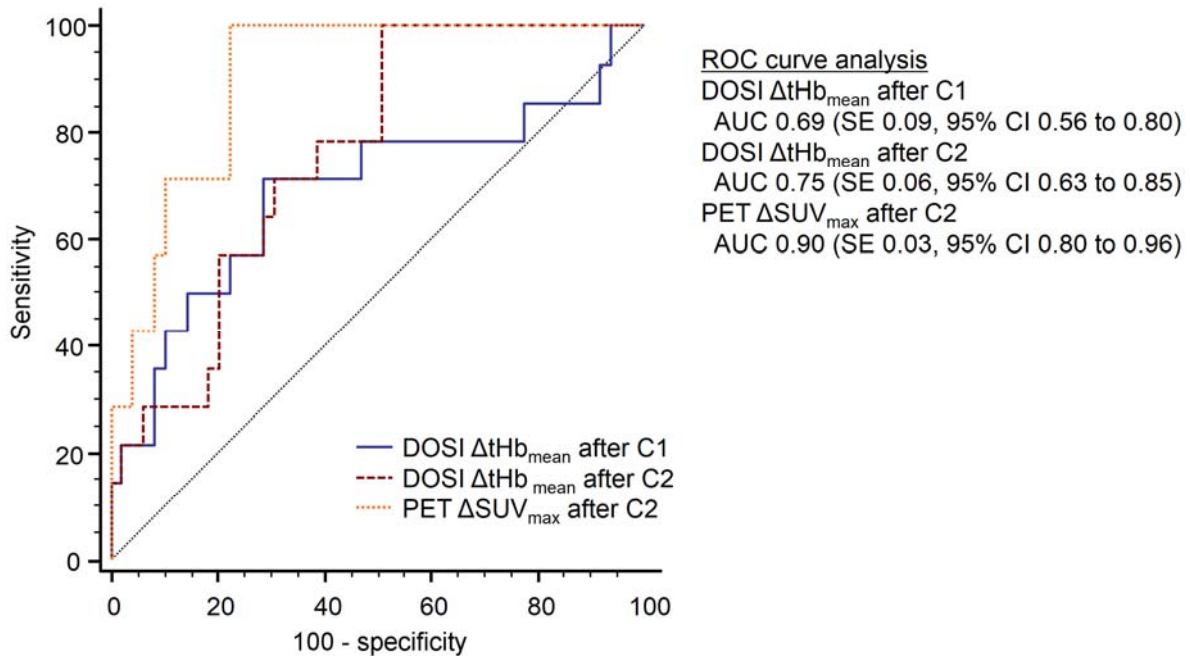


**Figure 4.** Comparison of the diagnostic performance between DOSI  $\Delta tHb_{mean}$  and FDG-PET  $\Delta SUV_{max}$  for predicting pCR. ROC curve analysis indicated AUC 0.69 of  $\Delta tHb_{mean}$  after C1, AUC 0.75 of  $\Delta tHb_{mean}$  after C2, and AUC 0.90 of  $\Delta SUV_{max}$ .  $\Delta tHb_{mean}$  after C1 was significantly inferior to  $\Delta SUV_{max}$  ( $p = 0.03$ ); there were no significant differences between  $\Delta tHb_{mean}$  after C2 and  $\Delta SUV_{max}$  ( $p = 0.06$ ) and between  $\Delta tHb_{mean}$  after C1 and  $\Delta tHb_{mean}$  after C2 ( $p = 0.2$ ). ROC, receiver operating characteristic; AUC, area under the curve; C1, the first chemotherapy course; C2, the second chemotherapy course; DOSI, diffuse optical spectroscopic imaging; FDG, 2-deoxy-2- $^{18}F$ -fluoro-D-glucose; PET, positron emission tomography; SUV, standardized uptake value;  $tHb_{mean}$ , mean value of the total hemoglobin concentration.

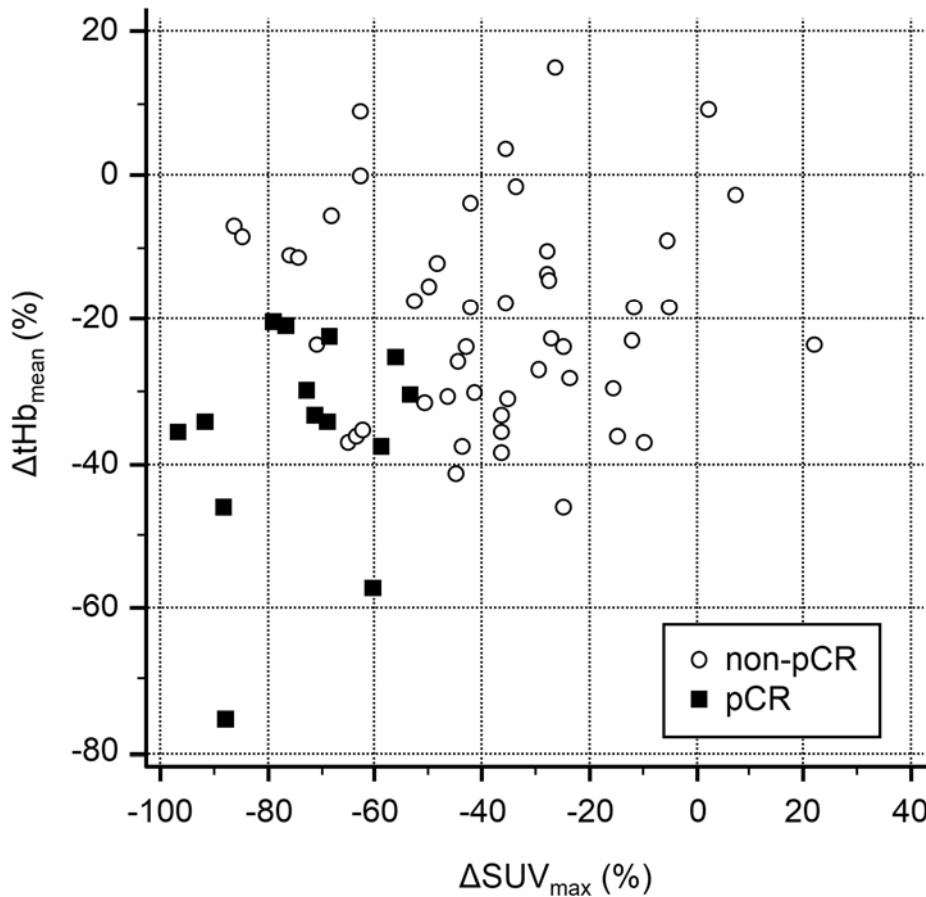


**Figure 5.** Scatter plots showed no significant linear correlation between FDG-PET  $\Delta\text{SUV}_{\text{max}}$  and DOSI  $\Delta\text{tHb}_{\text{mean}}$  ( $r = 0.23$ ; 95% CI,  $-0.01$  to  $0.45$ ,  $p = 0.06$ ). Results using the post-second-course  $\Delta\text{tHb}_{\text{mean}}$  and  $\Delta\text{SUV}_{\text{max}}$  with optimal cutoffs for pCR identification: sensitivity 100%; specificity 92.0%; PPV 77.7%; NPV 100%; accuracy 93.7%. Filled square, pCR; empty circle, non-pCR. DOSI, diffuse optical spectroscopic imaging; FDG, 2-deoxy-2- $^{18}\text{F}$ -fluoro-D-glucose; NPV, negative predictive value; pCR, pathological complete response; PET, positron emission tomography; PPV, positive predictive value; SUV, standardized uptake value;  $\text{tHb}_{\text{mean}}$ , mean value of the total hemoglobin concentration.



**Table 1.** Patient and tumor characteristics

Characteristic	DOSI study		DOSI + PET study	
	No. of patients	%	No. of patients	%
Total number	84		64	
Age, years				
Mean	56		55.9	
SD	10.4		11.4	
Range	35–77		35–77	
Tumor size (mm)				
Mean	37.5		39.3	
SD	16.8		17.1	
Range	7–97		7–97	
Histology				
IDC	76	90.5	56	87.5
ILC	2	2.4	2	3.1
Others	6	7.1	6	9.4
Estrogen receptor status				
Positive	47	55.9	37	57.8
Negative	37	44.1	27	42.2
Progesterone receptor status				
Positive	37	44.1	32	50
Negative	47	55.9	32	50
HER2 status				
Positive	18	21.4	14	21.9
Negative	66	78.6	50	78.1
Nodal status				
Positive	58	69	43	67.2
Negative	26	31	21	32.8
Histological assessment after NAC				
pCR ( <i>ypT0/is, ypN0</i> )	13	15.5	11	17.2
pCR ( <i>ypT0/is, ypN1</i> )	3	3.5	3	4.7
non-pCR	68	81	50	78.1

SD, standard deviation; IDC, invasive ductal carcinoma; ILC, invasive lobular carcinoma; NAC, neoadjuvant chemotherapy;

Table 2. Chemotherapy regimens

Type of regimen	No. of courses	No. of patients	%
Nab-paclitaxel 260 mg/m <sup>2</sup> , q3w	4	22	26.2
Followed by epirubicin 90 mg/m <sup>2</sup> + cyclophosphamide 600 mg/m <sup>2</sup> , q3w	4		
Epirubicin 90 mg/m <sup>2</sup> + cyclophosphamide 600 mg/m <sup>2</sup> , q3w	4	30	35.7
Followed by docetaxel 75 mg/m <sup>2</sup> , q3w	4		
Docetaxel 75 mg/m <sup>2</sup> + doxorubicin 50 mg/m <sup>2</sup> + cyclophosphamide 500 mg/m <sup>2</sup> , q3w	4	1	1.2
FU 500 mg/m <sup>2</sup> + epirubicin 90 mg/m <sup>2</sup> + cyclophosphamide 500 mg/m <sup>2</sup> , q3w	4	2	2.3
Followed by docetaxel 75 mg/m <sup>2</sup> , q3w	4		
FU 500 mg/m <sup>2</sup> + epirubicin 90 mg/m <sup>2</sup> + cyclophosphamide 500 mg/m <sup>2</sup> , q3w	4	4	4.8
Followed by docetaxel 75 mg/m <sup>2</sup> + trastuzumab 6 mg/m <sup>2</sup> , q3w*	4		
Carboplatin AUC6 + docetaxel 75 mg/m <sup>2</sup> + trastuzumab 6 mg/m <sup>2</sup> , q3w*	6	15	17.9
Paclitaxel 90 mg/m <sup>2</sup> , qw×3 + bevacizumab 10 mg/kg, q2w×2	6	10	11.9

Nab, nanoparticle albumin-bound; FU, fluorouracil. \* Initial dose of trastuzumab was 8 mg/m<sup>2</sup>.